

DRONE SOUNDS AND ENVIRONMENTAL SIGNALS – A FIRST REVIEW

Oliver Jokisch and Dominik Fischer

*Institute of Communications Engineering, HfT Leipzig, Germany
jokisch@hft-leipzig.de*

Abstract: The article describes our first analysis and development steps to extend an unmanned aerial vehicle (UAV, drone) with an intuitive user interface during agriculture operations. The targeted sound and speech signal processing, e.g. to enable command recognition, is elaborate due to rotor and other noises of a flying drone. The signal processing has to deal with different sound sources, such as noise which disturbs the analysis or useful signals like speech commands and acoustical events that characterize environmental objects. Currently, typical commercial drones are not equipped with microphones. Therefore, we test basic scenarios and measurement steps to directly record acoustic signals including noise at a flying drone with a simple Lavelier microphone in different recording positions. In the resulting audio database, we analyze the according effects of microphone position, flight maneuver and environment in the spectrogram and power-density spectrum. Expectedly, the blade passing frequency (BPF) and the associated harmonic components, which depend on the motor rotation speed, constitute the main influence. In a further step, based on drone-recorded speech signals, we filter the harmonic components to feed a commercial speech recognizer without training or adaptation to drone noise, at which we achieve a command recognition rate of 96.2 %.

1 Introduction

The success of drones in various application fields has led to increased noise emissions, which are often regarded as noise pollution [1], not only in Germany. The previous research therefore focused on the sound immission – e.g. by measurements of the sound pressure level [2, 3, 4] and by spectral analyses of overflight noise [5], usually at static positions [6]. The most studies of influence factors considered the number and type of rotor blades [6], the motor rotation speed [2] and specific differences between quad, tri or hexcopters [5]. Beyond, some effects of drone sounds on animals were investigated (e.g. [7]). The predominant consideration of noise immission for humans and their environment resulted in investigations with typically static measurement positions outside the drone.

Considering the sophisticated sensor technology and signal processing in drone systems, it is surprising that the potential of audio signal analysis directly at a drone or in the near field was not systematically analyzed so far. The processing of environmental information is primarily focused on electromagnetic signals and image processing, including object recognition with a variety of camera techniques, see e.g. [8].

During the last years, science, business and politics recognized the potential of drones in agriculture operations [9]. A subtask in our EU project “Collaborative strategies of heterogeneous robot activity at solving agriculture missions controlled via intuitive human-robot interfaces (HARMONIC)” within the “ERA.Net RUS Plus” program 2018–2020, is the control of a group of unmanned aerial vehicles (UAV, drone), which shall include an intuitive user interface during agriculture operations.

Whereas UAV-related image processing was intensively studied in civil and military environments, a targeted sound processing turns out to be challenging due to rotor and many other noises at flying drones [5, 6, 7]. It is necessary to distinguish between the sound sources, e.g. noise which disturbs the analysis and the classification of external signals such as speech commands, acoustical events (characterizing environmental objects) or other useful signals that even allow a characterization of drone operations or failures [4]. The typical, commercially available, small drones do not provide audio recording facilities, but possible applications of audio processing at the flying drone include interesting use cases, such as:

- Recognition of speech commands
- Classification of environmental sounds (e.g. alarm signal, traffic object or animal voice)
- Detection of flight situation or failures (combined with other sensor data)
- Active noise cancellation.

In this contribution we survey different test scenarios and measurement setups to directly record audio signals including noise at a small (flying) drone, DJI Mavic Pro [10], with the commercial Lavalier microphone Rode smartLav+ to simulate economically priced standard equipment. In a first step of the analysis [11], we created a small database for different microphone positions and test environments, and we then analyzed the according parameter influence on the spectrogram and power-density spectrum.

In terms of a feasibility study, we wanted to examine, whether audio signals can be analyzed adequately at drones and if there are specific sound characteristics or reproducible patterns. Furthermore, we describe a simple word recognition experiment for seven imaginary commands based on drone-recorded and noise-reduced signals. For this purpose, we used the Google Cloud Speech-to-Text API [12] without additional training or noise adaptation.

2 Experimental methods

In this section, we summarize selected research questions and test scenarios including the prerequisites and experimental settings from [11].

2.1 Recording equipment and setup

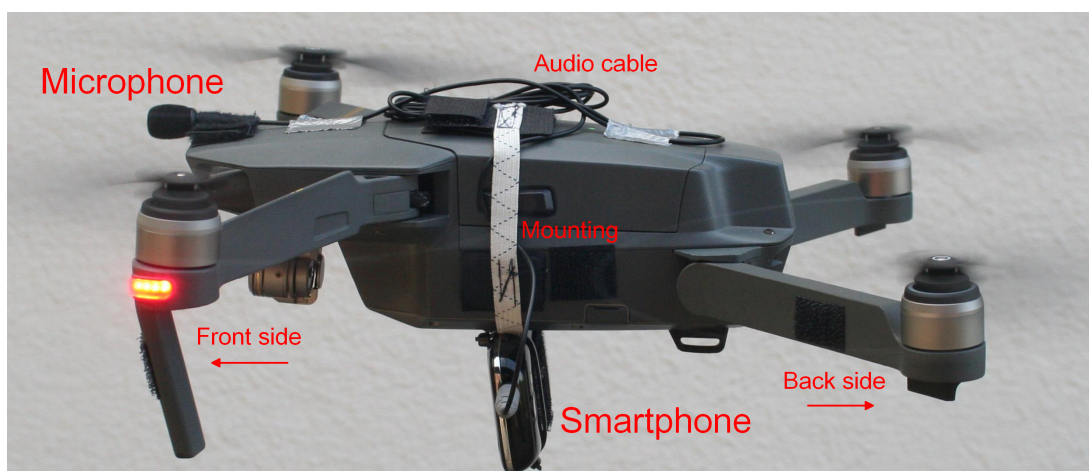


Figure 1 – Exemplary measurement setup with fixed microphone and recording smartphone from [11]

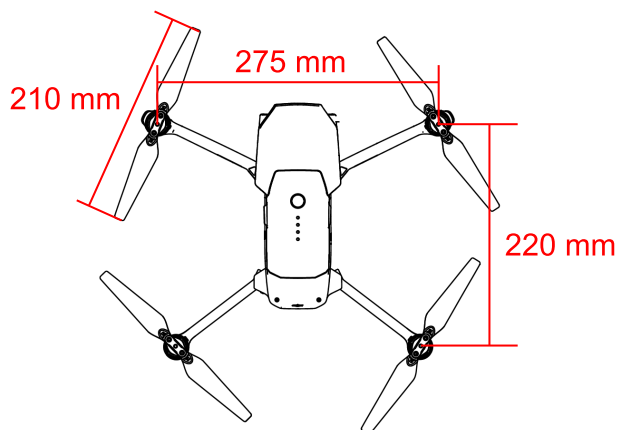


Figure 2 – Schematic top view of the drone dimensions from [10]

The used quadcopter drone DJI Mavic Pro weighs 734 g and provides a thrust-to-weight ratio (TTWR) of about 2.5 [13]. Figure 1 shows the drone and the recording equipment including mounting material (in total 102 g) – a single omnidirectional micro Rode smartLav+ (9 g, frequency range 20 Hz ... 20 kHz) connected to a hanging smartphone Jelly Pro (86 g). The additional drone weight of 13.9 % reduces the TTWR to ≈ 2.2 , which slightly degrades the flight quality. The Mavic drone can be interfolded for transport, so that there is no symmetry of front and back side. Besides, one can expect differences in the rotor-induced airstream above and below. To test different flight maneuvers, use cases or environments, we therefore recorded at the selected micro positions in Table 1. All positions varied in a maximal dimension of about 20 cm (cf. Figure 2). The smartphone was fixed in the center to ensure an appropriate weight distribution. Figure 3 visualizes the ten micro positions. All sounds were recorded at 44.1 kHz and 16 bit and stored in WAV format (linear PCM).

Table 1 – Overview about the microphone positions at the drone

Description	Abbreviation	Position numeral
above centered	CAbov	1
bottom centered	CBott	2
bottom left side	LBott	3
front centered	CFront	4
front, right side	RFront	5
back, right side	RBack	6
front, left side 1	LFront	7
back, left side 1	LBack	8
front, left side 2	LFront2	9
front, right side 2	RFront2	10

2.2 Maneuvers in flight and acoustic diagnostics

For a preliminary acoustic analysis, five basic maneuvers in flight can be considered (hovering, climb, dive, directional flight and rotation). Without external manipulation, a drone is hovering in a constant position by self-adapting the thrusts of the rotors, based on the sensor data. By increasing the motor rotation speed, the drone is forced to climb, and with decreased speed, the drone is diving. If the rotation speeds are reduced in both frontal engines, a directional forward flight can be achieved. Neighbored rotors are rotating reversely to compensate for the torque. By increasing the speeds of two opposing rotors with the same direction, the drone starts to rotate. Transitional phases between the maneuvers are characterized by non-stationary signals.

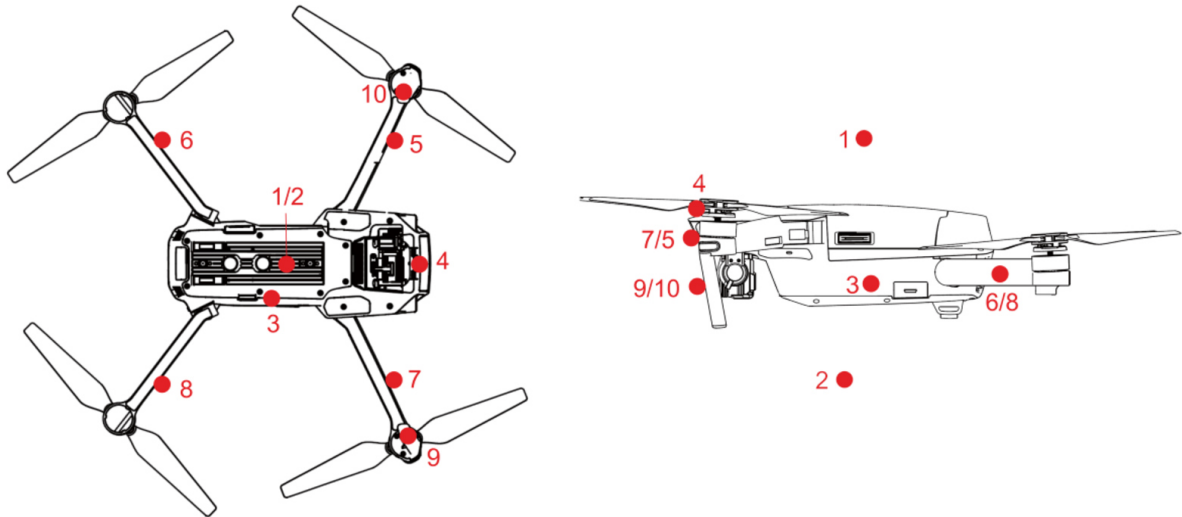


Figure 3 – Micro positions from Table 1 – bottom (left) and side view (right), based on [10]



Figure 4 – Imitated cracks in one of the rotor blades (on the right)

The major part of the emitted noise is associated with the rotor movement. To test the possibility of an acoustic flight diagnostics or damage prevention, we simulated a rotor defect by slightly cracking one rotor blade target-oriented as shown in Figure 4. The resulting flight maneuvers shall not be substantially influenced.

2.3 Flight environment and external sounds

Both, sensor technology and semi-automatic control of a commercial drone like Mavic limit the environmental test scenarios. For example, the crash protector prevents a close side-approach to walls, and the barrier detection starts to intervene already ≈ 30 cm over ground. Hence, we only recorded simple in and outdoor maneuvers like hovering under a concrete ceiling at micro 1 (above centered) or hovering over a wood plate, carpet, grassland or reed at micro 2 (bottom centered).

The decisive question for the use of drone-based audio signal processing is the chance of analyzing ambient signals in spite of drone or wind-induced noise, preferably without elaborate microphone technology (e.g. arrays). Exemplarily we have examined three scenarios:

- A passing (quiet) vehicle at 80 km/h on a country road – limousine BMW 5 series (E39)
- A passing (loud) vehicle at 30 km/h on a field – motocross motorcycle Yamaha JZF 250
- A loud and recurrent, tonal sound – ringing bell in a church tower.

The signals were recorded at the micro positions 2 and 4 (bottom centered or aside) and as favorable as possible, i.e. during hovering mode and in short distances of 1 . . . 5 m to the measured objects. The vehicles passed under the drone.

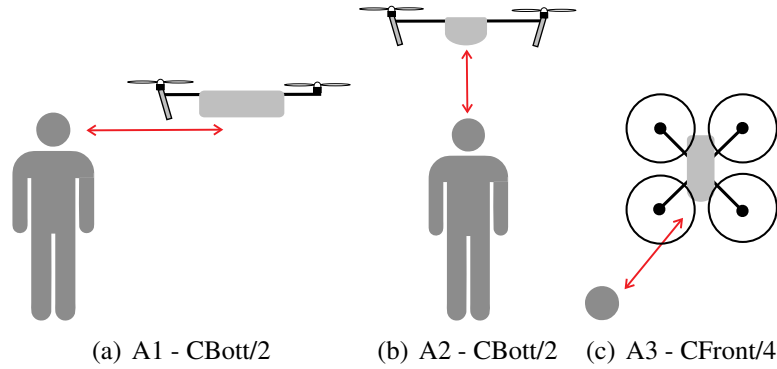


Figure 5 – Recording scenarios A1 ... A3 and micro positions for the command recognizer test

2.4 Speech recognizer, test data and pre-processing

Beside gestures, a speech control represents a potential task in a close-by human-drone interaction. For this purpose we played random sequences of the seven German commands “Halt”, “Stopp”, “Start”, “Fliege”, “Eins”, “Zwei” and “Drei”, prerecorded at 44.1 kHz, linear 16 bit (mono) from a male voice aged 22. To test different effects of rotor noise, microphone position and turbulent flow, we simulated three (loud)speaker positions with two speaker-microphone distances (SMD) of 0.5 and 1.0 m respectively, while the drone was hovering – as visualized in Figure 5. For demonstrating the effects of noise reduction, we used the ANR and notch-filter methods via Noise Gate from Audacity and GitHub respectively [14, 15] and a low-pass filtering with a cut-off frequency of 4 kHz. The drone-recorded command signals including the real-world noise and certain noise-reduced versions of each command were fed in random order to the Google Cloud Speech-to-Text API [12] without additional training or adaptation to the specific noise conditions [11].

In total, the database contains 735 command realizations – in average 14 signals per command for each of the three scenarios, including original and up to four noise-reduced versions.

3 Results and discussion

3.1 Spectral characteristics

A representative rotation speed in the hovering mode is about $6,000 \text{ min}^{-1}$. With two blades, the associated blade passing frequency (BPF) results in $f_{BP} = 2 \cdot f_{motor} = 2 \cdot 6,000/60 \text{ s} = 200 \text{ Hz}$. In Figure 6, the BPF and its dominant harmonics can be observed in the frequency range up to $\approx 3 \text{ kHz}$. The additional, characteristic peaks in the frequency ranges $3.9 \dots 4.4 \text{ kHz}$ and $6.5 \dots 7.5 \text{ kHz}$ are presumably related to interferences between the rotors (BPFs) and reflections, since there is no external sound source. The overall decline of the curve characterizes the frequency response of the microphone.

3.2 Influence of microphone position

In hovering mode, the expected signal differences between the micro positions 1 ... 3 (above centered versus bottom centered or aside) are less significant, at which the power density level in the frequency range of $2 \dots 6 \text{ kHz}$ is on average 5 dB lower at position 1, whereas the dominant harmonics increase by 5 dB at position 3, i.e., the previously assumed effects of air streams on the positions and audio signals seem to be small. In contrast, front and back recordings show reproducible differences, e.g. at micro position 8 (LBack) with a power density peak in the range of $6.5 \dots 7.5 \text{ kHz}$, which is about 15 dB higher than at position 7 (LFront). Recordings between

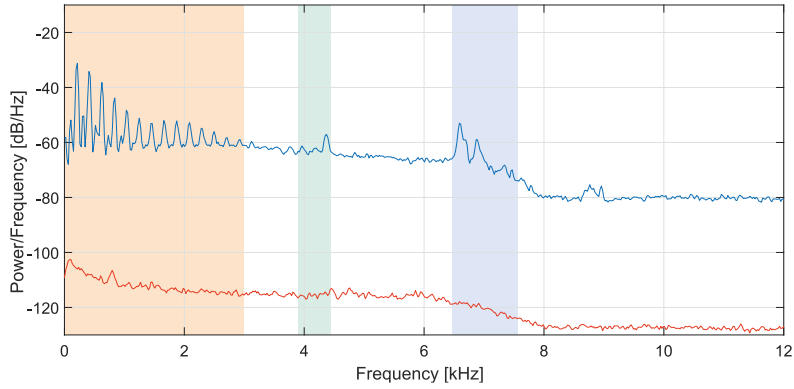


Figure 6 – Power density spectra of 2 seconds hovering at micro position 3 (upper curve) with dominant harmonics in a frequency range till ≈ 3 kHz vs. recording of silence (lower curve)

two rotors or close to a single rotor (position 9 or 10) reduce the influence and diversity (e.g. by varying rotation speeds) of other sound sources and thus lead to more reproducible spectra, which can ease a posterior filtering of disturbing noise.

3.3 Effects of flight maneuvers and drone speed

At the beginning of a climb, the rotation speeds are shortly increased for drone acceleration, before they turn back to the previous level, as demonstrated in Figure 7 within the time interval 1.1...2.5 s. The harmonic target frequencies in this example can be approximately calculated as follows: $f_{k,climb} = f_{k,hover} + k \cdot f_{shift}$. The measured values are summarized in Table 2, representing a shift of: $f_{shift} \approx 0.32 \cdot f_{0,hover} = 65$ Hz. In the two higher frequency ranges, the peaks are shifted approximately by the same factor (e.g. the peak at 4,285 Hz to $\approx 5,700$ Hz).

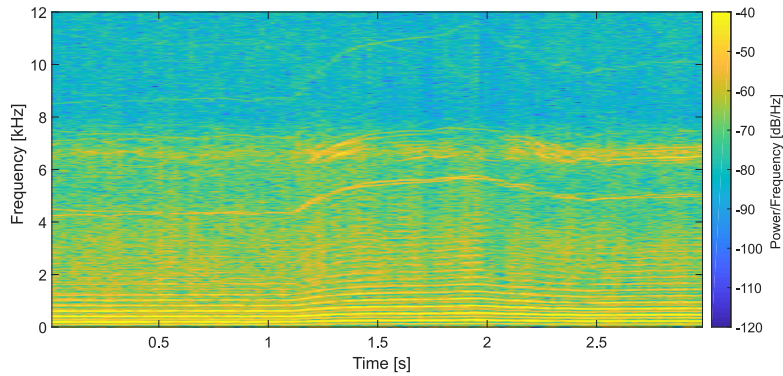


Figure 7 – Spectrogram of climbing (beginning at 1.1 s) for micro position 3 (bottom left)

Table 2 – Initial frequency shift at the climbing drone (measured values, rounded)

Harmonic k	$f_{k,hover}$ in Hz	$f_{k,climb}$ in Hz	$f_{k,shift}$ in Hz
1	205	270	65
4	840	1,100	260
5	1,040	1,360	320
6	1,250	1,630	380

The other maneuvers such as dive (negative frequency shift at the beginning) result in analog spectral effects, which also allow for an acoustic classification of the flight mode. In contrast, the speed of directional flight is mainly controlled by the orientation angle of the drone,

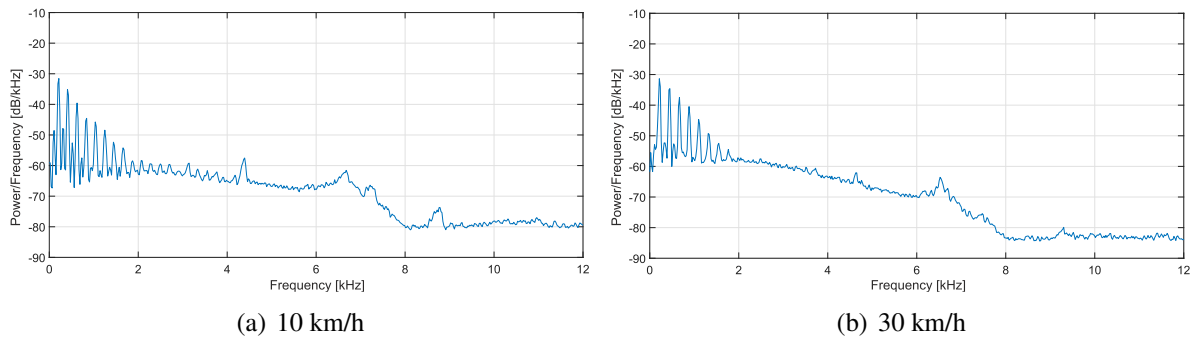


Figure 8 – Power density for different drone speeds at micro 3 (bottom left side) – directional flight, 2 s

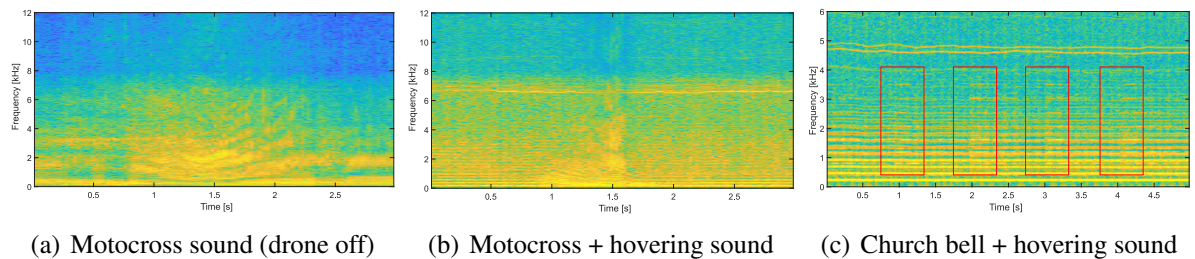


Figure 9 – Spectrograms of external sounds – motorcycle (dist. 1 m, mic. 2) and bell (5 m, mic. 4)

caused by slight modifications in the rotation differences only. Consequently, the power density spectra at the lower drone speeds 10 and 30 km/h look similar, cf. Figure 8. For higher speeds like 60 km/h (sport mode), the power density in the range till 2 kHz is rising considerably.

3.4 Flight environment, external sounds and rotor defect

By our experimental setup, we can not find reproducible spectral patterns related to the tested in and outdoor flight environments – even in short distances of 30...60 cm over ground or under ceiling. Although the recorded signals are effected by sound reflections and absorption, the spectra are presumably dominated by the influences of micro position and flight maneuver, as previously discussed.

The car sounds are almost completely masked by the drone sound, i.e., not really audible or detectable in the spectrogram, apart from a short level reduction, which is presumably caused by the air blast in the moment of passing. In contrast, the motocross sounds (Figure 9a/b) and also the bell-ringing (Figure 9c) can be still detected at close range.

The recordings of hovering maneuvers in position 8 (back, left side) close to the cracked rotor show small but not really reproducible changes in the power-density spectrum, compared to previous recordings with an intact rotor blade, cf. Figure 10.

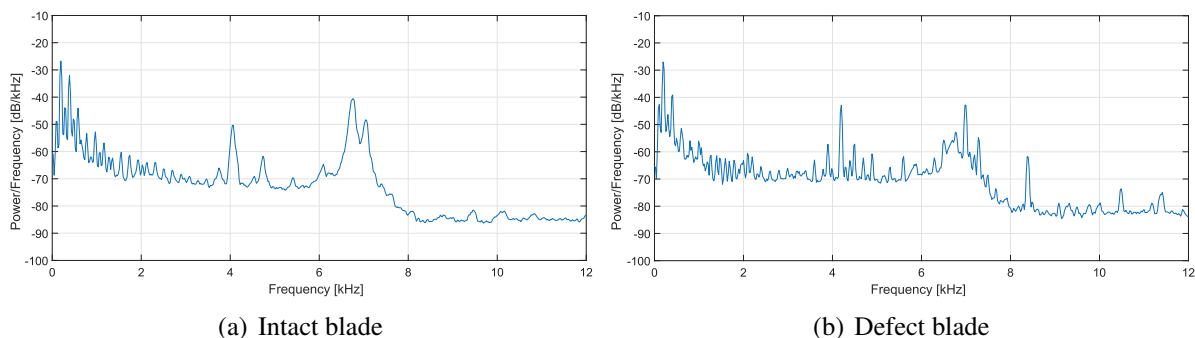


Figure 10 – Comparison of power-density spectra at micro position 8 – rotor blade intact vs. defect, 2 s

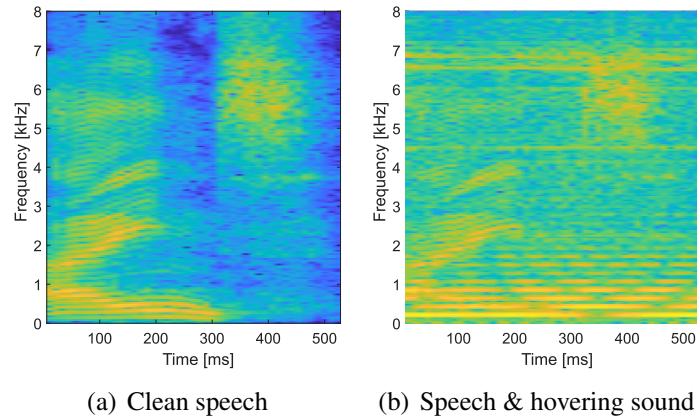


Figure 11 – Spectrogram of the command “Eins” at micro position 4 (front centered)

3.5 Recognition of speech commands

The results of the command recognition are indicative and shall illustrate the potential for the further studies only – the experimental details and more results are described in [11]. Expectedly, the harmonic components of both, speech and rotor sounds, overlap to a large extent, in particular in the frequency range till 2 kHz, as visualized in Figure 11. Already for a short SMD of 0.5 m, the signal-noise ratio (SNR) is 0 dB only, and a targeted, BPF-related filtering of the rotor sounds seems to be challenging. Table 3 summarizes the recognition rates (RR) for 343 command realizations at the best-possible speaker position (scenario A3 with 0.5 m distance), after applying different methods of noise reduction.

Table 3 – Overall recognition rate (RR) and rejections in scenario A3 (343 signals) with SMD \approx 0.5 m

Noise reduction	SNR in dB	Rejections in %	RR in %	RR w/o rejections in %
–	0	(100.0)	–	–
ANR	20	89.80	10.20	100.0
Notch & low pass	5	69.39	28.57	93.33
Notch & ANR	25	53.06	32.65	69.57
Notch-filtering	3	46.94	51.02	96.15

A command recognition without noise reduction is impossible, but although achieving an SNR improvement of 20 dB, also the ANR method can not provide adequate input signals for the non-adapted speech recognizer (rejection rate of 89.8 %). The notch-filtering seems to work in certain limits due to a targeted suppression of harmonics. Regardless of an unacceptable rejection rate of 46.9 %, the overall recognition rate exclusive rejections achieves 96.2 %.

4 Conclusions

As expected, most of the recordings show dominating blade passing frequencies (BPFs), which depend on the four motor rotation speeds, and their associated harmonic components. Further characteristic peaks can be observed in the frequency ranges 3.9...4.4 kHz and 6.5...7.5 kHz. The signal characteristics vary with recording position and flight maneuver. It is difficult to analyze sounds from environment. A simple command recognition, based on drone-recorded and noise-filtered signals without recognizer training or adaptation to the noise conditions, is possible. As a next step, we will study improved microphone constellations, e.g. a microphone array, rather than new or more complex user scenarios. The experiments will include sound recordings of an affixed drone in a semianechoic room to ensure reproducible conditions.

Acknowledgement

This work was supported by the EU project “Collaborative strategies of heterogeneous robot activity at solving agriculture missions controlled via intuitive human-robot interfaces (HARMONIC)” within the “ERA.Net RUS Plus / Robotics” program 2018–2020 (project ID 99) co-funded by the German Federal Ministry of Education and Research (BMBF) under Grant No. 01 DJ18011.

References

- [1] *Mögliche Probleme durch die Nutzung ziviler Drohnen in Deutschland im Jahr 2016*. July 2016. URL [de.statista.com/statistik/daten/studie/596521/umfrage/umfrage-zu-moeglichen-problemen-durch-die-nutzung-ziviler-drohnen](https://www.de.statista.com/statistik/daten/studie/596521/umfrage/umfrage-zu-moeglichen-problemen-durch-die-nutzung-ziviler-drohnen). Retrieved 31/10/2018.
- [2] PAPA, U., G. IANNACE, G. D. CORE, and G. GIORDANO: *Determination of sound power levels of a small uas during flight operations*. In *Proc. INTER-NOISE*, vol. 45, pp. 216–226. August 2016.
- [3] MIESIKOWSKA, M.: *Analysis of signal of x8 unmanned aerial vehicle*. In *Proc. IEEE Conf. Signal Processing: Algorithms, Architectures, Arrangements & Applications (SPA)*, pp. 69–72. Sept. 2017.
- [4] KLOET, N., S. WATKINS, and R. CLOTHIER: *Acoustic signature measurement of small multi-rotor unmanned aircraft systems*. *International Journal of Micro Air Vehicle*, 9(1)(7), pp. 3–14, February 2017. URL doi.org/10.1177/1756829316681868.
- [5] CABELL, R., F. GROSVELD, and R. MCSWAIN: *Measured noise from small unmanned aerial vehicles*. In *Proc. INTER-NOISE / NOISE-CON*, vol. 252, pp. 345–354. June 2016.
- [6] INTARATEP, N., W. ALEXANDER, W. DEVENPORT, S. GRACE, and A. DROPKIN: *Experimental study of quadcopter acoustics and performance at static thrust conditions*. In *Proc. Aeroacoustics Conference (AIAA/CEAS)*, vol. 22. June 2016.
- [7] ISLAM, R., A. STIMPSON, and M. CUMMINGS: *Small UAV noise analysis*. Technical report of Humans and Autonomy Laboratory, Duke University, Durham, NC, USA, 2017.
- [8] *Incorporating drones into your security System – How we currently use drones*. July 2018. URL netwatchsystem.com/blog/incorporating-drones-into-your-security-system. Retrieved 21/01/2019.
- [9] KERSTING, S.: *Digitalisierung und Subventionen – die neuen Baustellen der Landwirtschaft*. *Handelsblatt*, 16 January 2019. URL <https://www.handelsblatt.com/politik/deutschland/gruene-woche-digitalisierung-und-subventionen-die-neuen-baustellen-der-landwirtschaft-/23869602.html>. Retrieved 21/01/2019.
- [10] *DJI Mavic Pro*. 2018. URL <https://www.dji.com/en/mavic>. Retrieved 27/01/2019.
- [11] FISCHER, D.: *Untersuchung von Geräusch- und Sprachsignalen beim Einsatz von Flugdrohnen [UAV] (in German)*. Bachelor’s thesis, HfT Leipzig, Germany, November 2018.
- [12] *Fundamentals of Cloud Speech-to-Text*. Retrieved 24/10/2018. URL cloud.google.com/speech-to-text/docs/basics.
- [13] *Drone thrust testing*. Retr. 21/09/2018. URL www.halfchrome.com/drone-thrust-testing.
- [14] *How audacity noise reduction works*. Retrieved 11/11/2018. URL wiki.audacityteam.org/wiki/How_Audacity_Noise_Reduction_Works.
- [15] *Noisereduction.cpp*. Retrieved 30/10/2018. URL github.com/audacity/audacity/blob/master/src/effects/NoiseReduction.cpp.